DOI:10.1021/jf901308p

JOURNAL OF AGRICULTURAL AND FOOD CHEMISTRY
ARTICLE

Gallic Acid Induces Apoptosis via Caspase-3 and Mitochondrion-Dependent Pathways in Vitro and Suppresses Lung Xenograft Tumor Growth in Vivo

Bin-Chuan Ji,[†] Wu-Huei Hsu,[§] Jai-Sing Yang,[#] Te-Chun Hsia,[§,⊥] Chi-Cheng Lu,[∥] Jo-Hua Chiang,[∥] Jiun-Long Yang,[⊗] Ching-Hsiung Lin,[†] Jen-Jyh Lin,[⊥,+] Lee-Jen Wu Suen,[†] Wellington Gibson Wood,[△] and Jing-Gung Chung*[,★,◇]

[†]Division of Chest Medicine, Department of Internal Medicine, Changhua Christian Hospital, Changhua 500, Taiwan, [§]Department of Internal Medicine, China Medical University, Taichung 404, Taiwan, [#]Department of Pharmacology, [⊥]Graduate Institutes of Chinese Medical Science, China Medical University, Taichung 404, Taiwan, [∥]Department of Life Sciences, National Chung Hsing University, Taichung 402 Taiwan, [⊗]Graduate Institute of Chinese Pharmaceutical Science, China Medical University, Taichung 404, Taiwan, [+]Division of Cardiology, China Medical University Hospital, Taichung 404, Taiwan, [△]Department of Pharmacology, School of Medicine and Geriatric Research, Education and Clinical Center, VA Medical Center, University of Minnesota, Minneapolis, Minnesota 55417, [★]Department of Biological Science and Technology, China Medical University, Taichung 404, Taiwan, and [◇]Department of Biotechnology, Asia University, Taichung 413, Taiwan

Several studies have shown that gallic acid (GA) induces apoptosis in different cancer cell lines, whereas the mechanism of action of GA-induced apoptosis at the molecular level in human non-small-cell lung cancer NCI-H460 cells is not well-known. Here, GA decreasing the percentage of viable NCI-H460 cells was investigated; GA-induced apoptosis involved G2/M phase arrest and intracellular Ca^{2+} production, the loss of mitochondrial membrane potential ($\Delta\Psi_m$), and caspase-3 activation. The efficacious induction of apoptosis and DNA damage was observed at 50−500 μM for 24 and/or 48 h as examined by flow cytometry, DAPI staining, and Comet assay methods. Western blotting and flow cytometric analysis also demonstrated that GA increased protein levels of GADD153 and GRP78, activation of caspase-8, -9, and -3, loss of $\Delta\Psi_m$ and cytochrome *c*, and AIF release from mitochondria. Moreover, apoptosome formation and activation of caspase cascade were associated with apoptotic cell death. GA increased Bax and Bad protein levels and decreased Bcl-2 and Bcl-xL levels. GA may also induce apoptosis through a caspase-independent AIF pathway. In nude mice bearing NCI-H460 xenograft tumors, GA inhibited tumor growth in vivo. The data suggest that GA induced apoptosis in NCI-H460 lung cancer cells via a caspase-3 and mitochondrion-dependent pathway and inhibited the in vivo tumor growth of NCI-H460 cells in xenograft models.

KEYWORDS: Gallic acid; apoptosis; caspase-3; mitochondria membrane potential ($\Delta\Psi_m$); NCI-H460 lung cancer cells; xenograft tumors

INTRODUCTION

Cancer is a major cause of death throughout the world. In the United States and western Europe, lung cancer is the leading cause of cancer death in men and women (*1*−*3*). In Taiwan, lung cancer also is the major cause of cancer-related deaths (*4*, *5*), and about 34.9 persons per 100000 die annually from lung cancer on the basis of reports from the Department of Health, Executive Yuan, ROC (Taiwan). The treatment of lung cancer includes surgery, radiation, chemotherapy, or a combination of radiotherapy and chemotherapy; however, mortality remains high after those treatments. It is recognized that chemoprevention is the use of pharmacological or natural agents to inhibit the development of cancer, and it is also well-known that chemoprevention can prevent a wide variety of cancers in multiple animal models (*6*). Moreover, many naturally occurring substances are thought to act as antioxidants and cancer preventative agents or even as cancer therapy drugs (*7*).

Gallic acid (3,4,5-trihydroxybenzoic acid, GA), a naturally occurring plant phenol, comes from the hydrolysis of tannins, and it has been shown to induce apoptosis in human leukemia HL-60RG cells (*8*) and many human cancer cell lines as well as human stomach cancer KATO III and colon adenocarcinoma COLO 205 cell lines (*8*). GA has been reported to play an important role in the prevention of malignant transformation (*9*), and GA was shown to have antitumor effects on LL-2 lung cancer cells transplanted in mice (*10*). GA induces apoptosis in human lung cancer cells (*11*), but the possible molecular mechanism of

*Corresponding author (telephone +886 4 2205 3366, int. 2161; fax +886 4 2205 3764; e-mail jgchung@mail.cmu.edu.tw).

 Published on Web 07/27/2009

apoptosis in human lung cancer NCI-H460 cells still is not clear. Therefore, it is important to clarify the in vitro anti-lung cancer activity of GA and also to find the possible signaling pathway. In the present study, the effects of GA were investigated using the growth of human lung cancer NCI-H460 cells in vitro and in vivo.

MATERIALS AND METHODS

Chemicals and Reagents. Gallic acid (GA), dimethyl sulfoxide (DMSO), propidium iodide (PI), RNase A, and Triton X-100 were obtained from Sigma Chemical Co. (St. Louis, MO). RPMI-1640, penicillin−streptomycin, trypsin−EDTA, fetal bovine serum (FBS), and L-glutamine were obtained from Gibco BRL (Grand Island, NY). Caspase-3, caspase-8, and caspase-9 activity assay kits were from OncoImmunin, Inc. (Gaithersburg, MD).

Human Lung Carcinoma Cell Line (NCI-H460). NCI-H460 cell line was obtained from the Food Industry Research and Development Institute (Hsinchu, Taiwan). The cells were plated in 75 cm^2 tissue culture flasks in RPMI-1640 medium supplemented with 10% FBS, 2 mM L-glutamine, 100 units/mL penicillin, and 100 μg/mL streptomycin. Cells were grown at 37 °C under humidified 5% CO_2 and 95% air at 1 atm (*12*−*14*).

Assessment of Cell Morphology and Viability. Approximately 2×10^5 cells/well of NCI-H460 cells were plated onto 12-well plates and incubated at 37 °C for 24 h before being treated with 0, 100, 200, 300, 400, and 500 μM GA and then incubated for 24 and 48 h. DMSO (solvent) was used for the control regimen. For cell morphology, cells were examined and photographed under a phase-contrast microscope. For percentage of cell viability, cells (1×10^5 cells per sample) were centrifuged at 1000*g* for 5 min, cell pellets were dissolved with 0.5 mL of PBS containing 100 μg/mL RNase, and 5 μg/mL propidium iodide, and viable cells were determined by using a flow cytometer (Becton-Dickinson, San Jose, CA) as previously described (*15*, *16*).

Determinations of Cell Cycle and Apoptosis by Flow Cytometry. Approximately 2×10^5 cells/well of NCI-H460 cells were grown on a 12-well plate for 24 h after which different concentrations of GA (0, 50, 100, 150, and 200 μM) were added, and cells were incubated at 37 °C in 5% CO_2 and 95% air for 48 h. For cell cycle arrest with sub-G1 (apoptosis), isolated cells were fixed by 70% ethanol in 4 °C overnight and then resuspended in PBS containing 40 μg/mL PI and 0.1 mg/mL RNase and 0.1% Triton X-100 in a dark room for 30 min at 37 °C. Those cells were analyzed with a flow cytometer equipped with an argon ion laser at 488 nm wavelength. The cell cycle with sub-G1 (apoptotic cells) was then determined, and analysis was conducted with FACScalibur utilizing CellQuest software (Beckton Dickinson) (*15*−*17*).

Comet Assay for DNA Damage. The Comet assay was done according to the procedures of Wang et al. with some modifications (*18*). The NCI-H460 cells were incubated with 0, 100, 200, 300, 400, and 500 μM GA, 0.5% H_2O_2, and vehicle (DMSO) for 24 h. Cells were harvested for the examination of DNA damage using the Comet assay as described elsewhere. Comets of cells on slides acquired DNA damage by using the CometScore Freeware analysis (TriTek Corporation, Sumerduck, VA). Comet tail length was calculated, quantified, and expressed as the mean ± SD (*16*, *18*, *19*).

DAPI Staining for Apoptotic Cells. NCI-H460 cells at a density of 2×10^5 cells/well were plated onto 6-well plates and incubated for 48 h before cells from each sample were isolated for 4,6-diamidino-2-phenylindole dihydrochloride (DAPI) staining, as described previously (*15*, *16*). After staining, the cells were examined and photographed using a fluorescence microscope (*15*).

CDK1 Activity Assay. CDK1 kinase activity was analyzed according to the protocol of the Medical and Biological Laboratories CDK1 kinase assay kit (MBL). In brief, NCI-H460 cells at a density of 2×10^6 cells/well were plated onto 6-well plates and were incubated with 250 μM GA for 0, 3, 6, 12, and 24 h. About 1×10^6 cells were suspended in a buffer of 0.2 mL (50 mM Tris-HC1, pH 7.5, 1 mM phenylmethanesulfonyl fluoride, 50 pg/mL leupeptin, 10 mM 2-mercaptoethanol, 1 mM MgCl, 2 mM EGTA, 0.5 mM dithiothreitol, 0.01% Brij35, 25 mM glycerophosphate, and 0.5 M NaCl). Cell suspensions were then sonicated and centrifuged at 100000*g* for 30 min. To determine the adequate cdc2 kinase assay condition using vimentin *MV55* peptide, cdc2 kinase assays were done with varying concentrations of vimentin *MV55* peptides (0.1−5 mM) and purified cdc2 kinase (*20*).

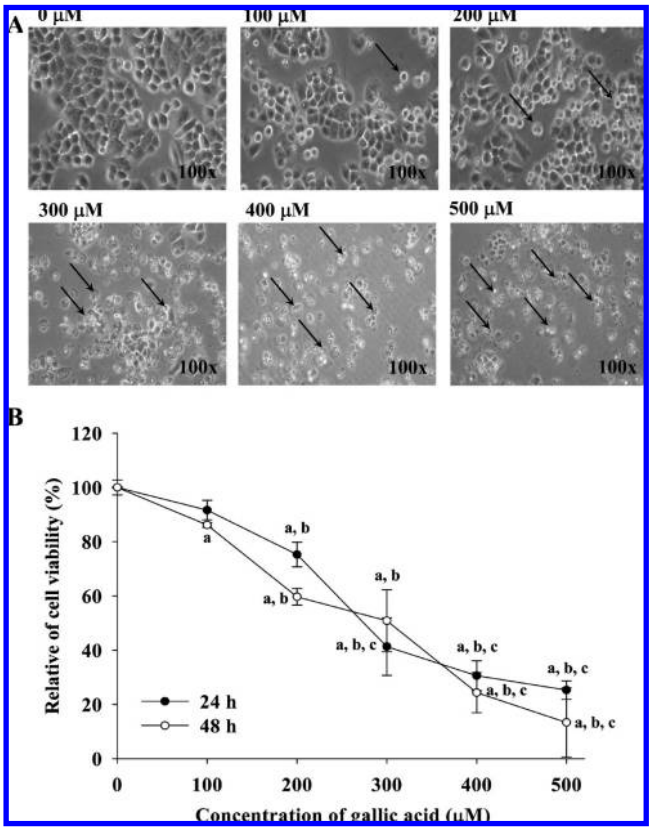

Figure 1. Effects of GA on the morphological changes and percentage of viable NCI-H460 cells. Cells were plated onto RPMI-1640 medium + 10% FBS with various concentrations of GA for 24 and 48 h, and the morphological changes were examined and photographed under phase-contrast microscope (**A**) (200×); total percentage of viable cells was determined by flow cytometry (**B**) as described under Materials and Methods. Each point is the mean ± SD of three experiments: a, $P < 0.05$, significantly different compared with DMSO-treated control; b, $P < 0.05$, significantly different compared with 200 μM GA treatment; c, $P < 0.05$, significantly different compared with 300 μM GA treatment by one-way ANOVA followed by Bonferroni's multiple-comparison test.

Reactive Oxygen Species (ROS), Intracellular Ca^{2+} Concentrations, and Mitochondrial Membrane Potential ($\Delta\Psi_m$) Determinations. NCI-H460 cells at a density of 2×10^5 cells/well were plated onto 12-well plates and treated with or without 250 μM GA for 0, 3, 6, 12, and 24 h to determine changes in ROS, intracellular Ca^{2+} concentrations, and $\Delta\Psi_m$. The endogenous ROS level, Ca^{2+}, and $\Delta\Psi_m$ were detected by flow cytometry using DCHF-DA, Fluo-3/AM, and $DiOC_6$. Cells were harvested and then resuspended in 500 μL of DCFH-DA (10 μM) for ROS (H_2O_2) determination, resuspended in 500 μL of Fluo-3/AM (2.5 μg/mL) for intracellular Ca^{2+} concentrations, and suspended in 500 μL of $DiOC_6$ (4 μmol/L) for $\Delta\Psi_m$ and incubated at 37 °C for 30 min and analyzed by flow cytometry (*21*−*23*). ROS levels, intracellular Ca^{2+}, and $\Delta\Psi_m$ were detectable in the FL-1 channel (a BD instrument with emission at 525 nm). All fluorescence intensities were obtained from the mean intensity of the histogram constructed from 10000 cells (*21*−*23*).

Caspase- 3, -8, and -9 Activity Determinations by Flow Cytometry. NCI-H460 cells at a density of 2×10^5 cells/well were plated onto 12-well plates, then pretreated with or without caspase-8 inhibitor (Z-IETD-FMK), caspase-9 inhibitor (Z-LEHD-FMK), or caspase-3 inhibitor (Z-DEVD-FMK) (R&D Systems, Minneapolis, MN), and then treated with 250 μM GA for 0, 6, 12, and 24 h. Cells were harvested by centrifugation, and the cell pellets were added to 50−75 μL of 10 mM caspase-3, -8, or -9 substrate solution (PhiPhiLux-G_1D_2, CaspaLux9-M_1D_2, CaspaLux8-L_1D_2). The samples were incubated in a 5% CO_2

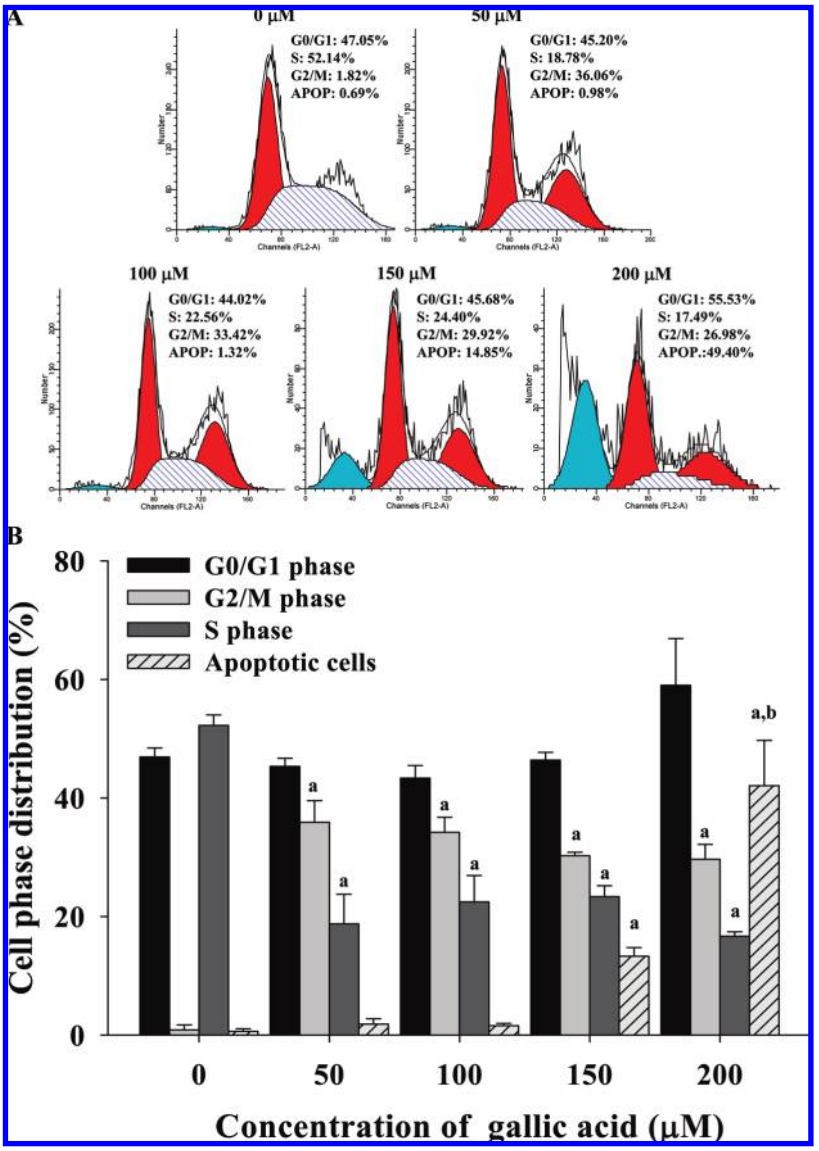

Figure 2. Effects of GA on the cell cycle and sub-G1 group of NCI-H460 cells. Cells were plated in RPMI-1640 medium + 10% FBS with various concentrations of gallic acid for 48 h, and the cells were analyzed for cell cycle (**A**, representative profiles; **B**, percentage of cells in phase) by flow cytometry. Each point is the mean ± SD of three experiments: a, $P < 0.05$, significantly different compared with DMSO-treated control; b, $P < 0.05$, significantly different compared with 150 μM GA treatment by one-way ANOVA followed by Bonferroni's multiple-comparison test.

incubator at 37 °C for 60 min before flow cytometric analysis. Caspase-3, -8, and -9 activities were detectable in the FL-1 channel (a BD instrument with emission at 525 nm) (*24*−*26*).

Apoptotic-Associated Proteins Examined by Western Blotting. A total of 5×10^5 NCI-H460 cells/mL cells were treated with 250 μM GA for 0, 6, 12, 24, and 48 h. Cells were then harvested from each sample by centrifugation for the total protein determination for Western blotting. Cytochrome *c*, Apaf-1, AIF, caspase-9, caspase-3, GADD153, GRP78, Fas, FasL, FADD, caspase-8, Bad, Bax, Bcl-2, and Bcl-xL expressions were examined using sodium dodecyl sulfate−polyacrylamide gel electrophoresis (SDS-PAGE) and Western blotting as described previously (*17*, *27*, *28*).

Real-Time PCR of Caspase-3 and -8. Total RNA was extracted from the NCI-H460 cells after treatment with 250 μM GA for 24 and 48 h, using the Qiagen RNeasy Mini Kit as described previously (*16*). RNA samples were reverse-transcribed for 30 min at 42 °C with the High-Capacity cDNA Reverse Transcription Kit (Applied Biosystems). Quantitative PCR was performed using the following conditions: 2 min at 50 °C, 10 min at 95 °C, and 40 cycles at 15 s at 95 °C, 1 min at 60 °C using 1 μL of the cDNA reverse-transcribed as described above, 2× SYBR Green PCR Master Mix (Applied Biosystems) and 200 nM forward (F) and reverse primers (R): caspase-3-F, CAGTGGAGGCCGACTTCTTG; caspase-3-R, TGGCACAAAGCGA CTGGAT; caspase-8-F, GGATGGCCACTGTGAATAACTG; caspase-8-R, TCGAGGACATCGCTCTCTCA; GAPDH-F, ACACCCACTCCTCCACCTTT; GAPDH-R, TAGCCAAATTCGTTGTCATACC. Each assay was run on an Applied Biosystems 7300 Real-Time PCR system in triplicate, and expression fold-changes were derived using the comparative C_T method (*16*).

NCI-H460 Xenograft Models. Eighteen female athymic BALB/$c^{nu/nu}$ nude mice (4−6 weeks of age) were obtained from the Laboratory Animal Center of National Applied Research Laboratories (Taipei, Taiwan). All mice were fed commercial diet and water ad libitum. NCI-H460 cells were resuspended in serum-free RPMI-1640 medium with Matrigel basement membrane matrix at a 5:1 ratio. The cell suspension (1×10^7 cells; total volume, 0.2 mL) was subcutaneously injected into the flanks of mice. Body weight and tumor mass were determined every 4 days. Animals with tumors were randomly assigned to one of three treatment groups [injected intraperitoneally every 4 days with 20 μL of DMSO control vehicle; GA (20 mg/kg); and doxorubicin (8 mg/kg)]. Treatment was initiated when xenografts reached volumes of about 100 mm^3. The tumor volume was estimated according to the following formula: tumor volume (mm^3) = $L \times W^2/2$ (L, length; W, width). At the end of the study, animals were sacrificed. Tumors were removed, measured, and weighed individually as described previously, and caspase-3, -8, and -9 activities were determined individually as described previously (*29*, *30*).

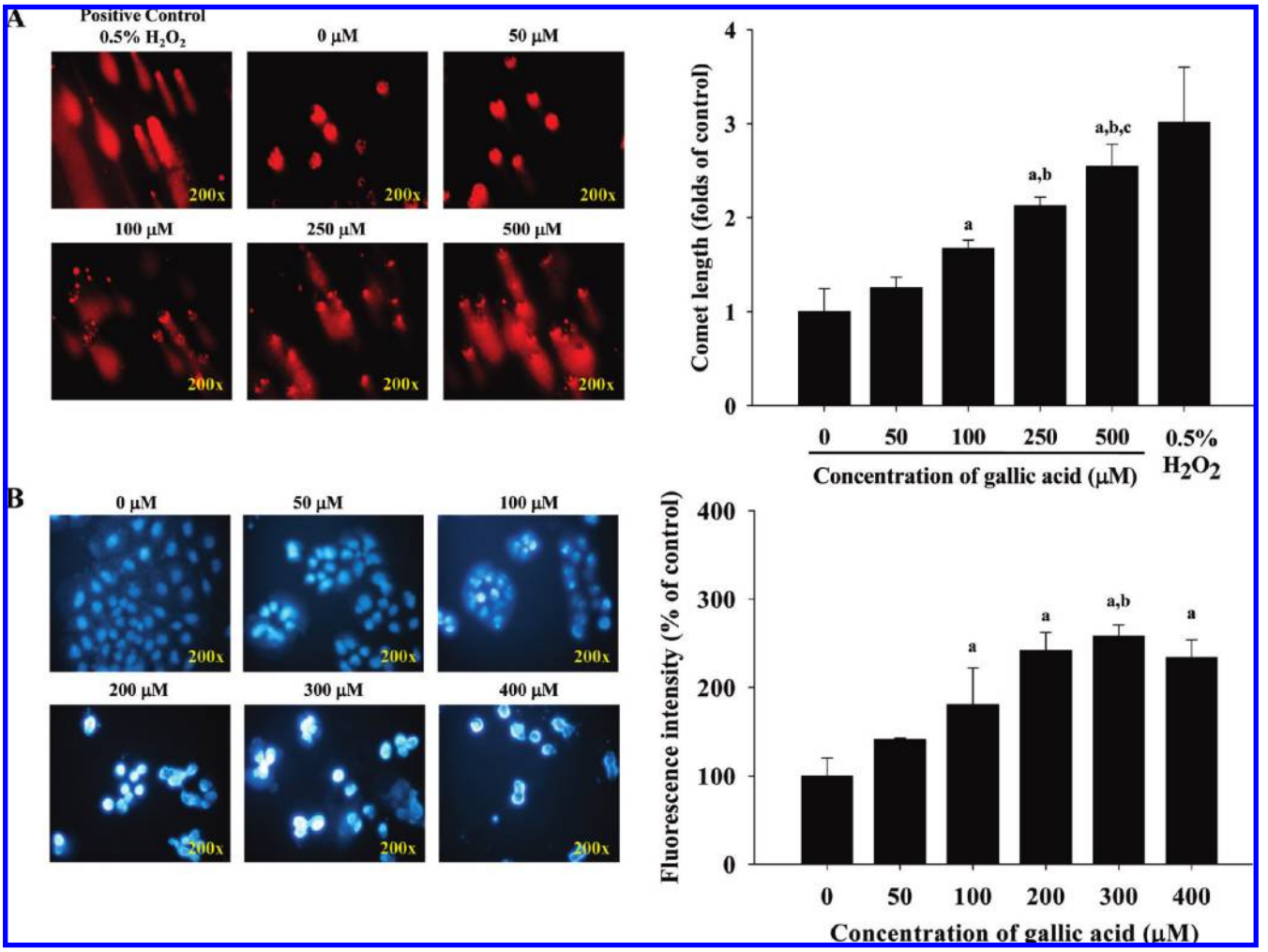

Figure 3. GA-induced DNA damage and apoptosis in NCI-H460 cells. Cells were incubated with various concentrations of gallic acid or 0.5% H_2O_2 for 24 h. DNA damage was determined using Comet assay and then monitored and photographed by fluorescence microscope (**A**); apoptotic cells were determined by DAPI staining and were photographed via fuorescence microscopy (**B**), which is described under Materials and Methods. (**A**) Each experiment was done with triple sets: a, $P < 0.05$, significantly different compared with DMSO-treated control; b, $P < 0.05$, significantly different compared with 100 μM GA-treated; c, $P < 0.05$, significantly different compared with 250 μM GA treatment by one-way ANOVA followed by Bonferroni's multiple-comparison test. (**B**) Each experiment was done with triple sets: a, $P < 0.05$, significantly different compared with DMSO-treated control; b, $P < 0.05$, significantly different compared with 200 μM GA treatment by one-way ANOVA followed by Bonferroni's multiple-comparison test.

Statistical Analysis. One-way ANOVA was used to examine the significance of differences in measured variables between control and treated groups followed by Bonferroni's test for multiple comparisons. Significance was declared at $P < 0.05$.

RESULTS

Effects of GA on Morphological Changes and Percent Cell Death. To examine the biological effects of GA, NCI-H460 cells were treated with various doses of GA (0, 100, 200, 300, 400, and 500 μM) for 24 and 48 h, and cell morphological changes and cell death were assayed. GA caused both cell morphological changes and cell death at a concentration of 100 μM or higher, which was dose-dependent (**Figure 1**). According to these results, we selected the 250 μM dose and next assessed whether the growth-inhibitory and cell death effects of GA are accompanied by its effect on cell cycle progression and/or apoptotic cell death.

Effects of GA on Cell Cycle and Sub-G1 Group of NCI-H460 Cells. GA induced significant cell cycle arrest at 50−200 μM after incubation for 24 h (**Figure 2**). Compared with DMSO controls, GA caused an arrest at G2-M (2 versus 26.98−36.06% $P < 0.001$, respectively) phase, which was at the expense of a strong decrease in the S-phase cell population (**Figure 2B**). GA at concentrations of 50−200 μM for 24 h caused significant apoptotic cell death. The increase in the percentage of sub-G1 indicated an increase in the percentage of apoptotic cells (**Figure 2B**), and this effect was dose-dependent.

GA-Induced DNA Damage and Apoptotic Cell Death in NCI-H460 Cells. To examine whether or not GA induced DNA damage in NCI-H460 cells, the Comet assay was used. GA induced DNA damage on the basis of the DNA damage tail production shown in **Figure 3A**. Further support for the role of apoptosis is that DAPI staining assays revealed that apoptotic cells were observed in GA-treated NCI-H460 cells compared with intact control cells, and this effect was dose-dependent (**Figure 3B**).

GA Affected the Levels of CDK1 Activity, Reactive Oxygen Species (ROS), Intracellular Ca^{2+}, and Mitochondria Membrane Potential ($\Delta\Psi_m$) in NCI-H460 Cells. To examine whether GA induced G2/M arrest, DNA damage, and apoptosis in NCI-H460 cells due to the effects of CDK1 activity, ROS, intracellular Ca^{2+}, and $\Delta\Psi_m$, NCI-H460 cells were exposed to 250 μM GA for various time periods. Our data demonstrated that GA induced

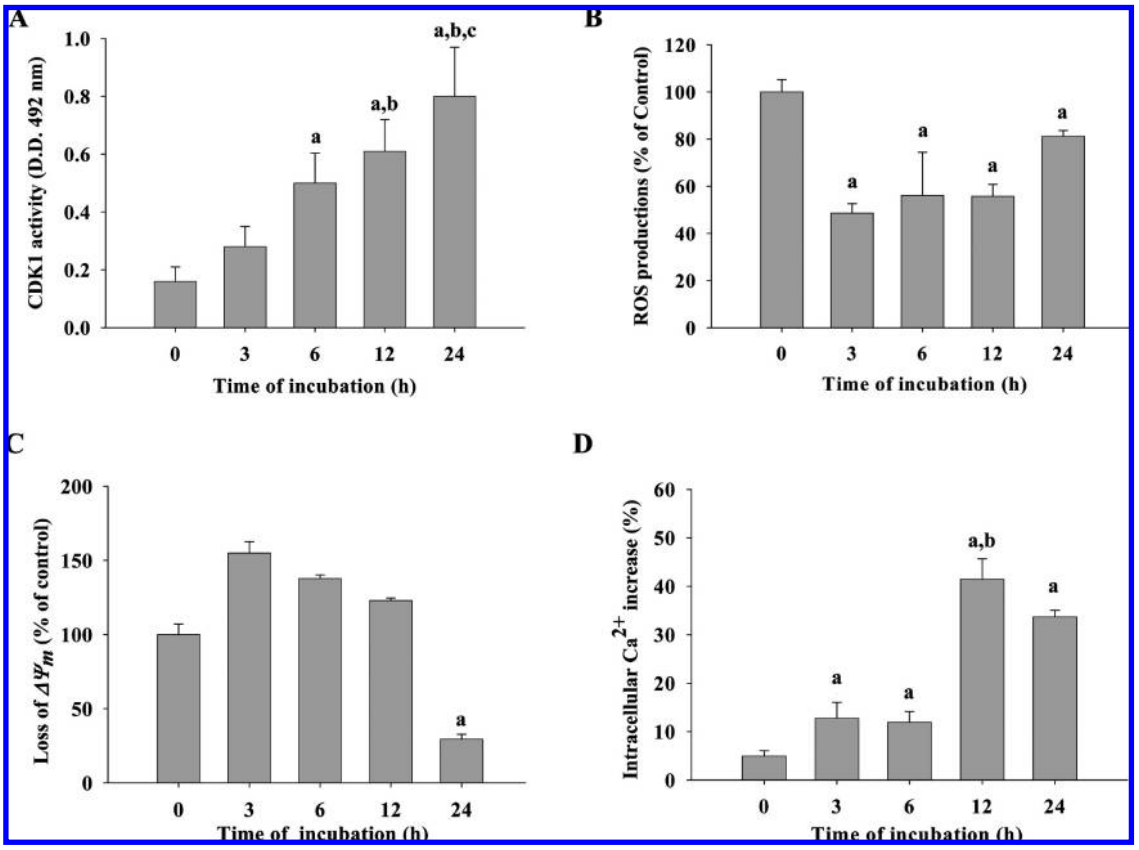

Figure 4. GA affected the levels of CDK1 activity, reactive oxygen species (ROS), and intracellular Ca^{2+} and mitochondria membrane potential ($\Delta\Psi_m$) in NCI-H460 cells. Cells were incubated with 250 μM GA for 0, 3, 6, 12, and 24 h for CDK1 activity (**A**), before staining by DCFH-DA for determination of ROS levels (**B**), stained with $DiOC_6$ for determination of the $\Delta\Psi_m$ levels (**C**), and stained by Fluo-3/AM for determination of the intracellular Ca^{2+} levels (**D**) by flow cytometric analysis as described under Materials and Methods. (**A**) Each experiment was done with triple sets: a, $P < 0.05$, significantly different compared with 0 time treatment by one-way ANOVA followed by Bonferroni's multiple-comparison test. (**B**) Each experiment was done with triple sets: a, $P < 0.05$, significantly different compared with 0 time GA treatment by one-way ANOVA followed by Bonferroni's multiple-comparison test. (**C**) Each experiment was done with triple sets: a, $P < 0.05$, significantly different compared with 0 time treatment; b, $P < 0.05$, significantly different compared with 6 h GA treatment by one-way ANOVA followed by Bonferroni's multiple-comparison test.

CDK1 activity in a time-dependent manner (**Figure 4A**). GA did not induce ROS production (**Figure 4B**); however, GA promoted the loss of $\Delta\Psi_m$ in NCI-H460 cells, and this effect also was time-dependent (**Figure 4C**). The results also showed that GA-induced levels of intracellular Ca^{2+} were slightly increased up to 12 h treatment, leading to the production of high levels of intracellular Ca^{2+}; after 24 h of treatment, the levels of Ca^{2+} started to decrease (**Figure 4D**).

GA Activated Caspase-3, -8, and -9 in NCI-H460 Cells. Caspase activation was examined in NCI-H460 cells, which were pretreated with or without inhibitors and then were treated with or without GA. Data in **Figure 5A−C** indicate that GA promoted activation of caspase-8, -9, and -3 in NCI-H460 cells, and these effects were time-dependent. **Figure 5D** indicates that all inhibitor pretreatments led to increase in the percentage of viable NCI-H460 cells.

GA Effected on Apoptosis-Associated Proteins in NCI-H460 Cells. Results from Western blotting are present in **Figure 6A−D**. GA stimulated levels of cytochrome *c* and AIF (**Figure 6A**), GADD153 and GRP78 (**Figure 6B**), Fas, FasL, FADD, and the active form of caspase-8 (**Figure 6C**), and Bad and Bax (**Figure 6D**), but decreased levels of pro-caspae-9 and -3 (**Figure 6A**) and Bcl-2 and Bcl-xL (**Figure 6D**) in NCI-H460 cells.

GA Inhibited Tumor Size in a Xenograft Mouse Model. On the basis of our in vitro studies, we next examined the in vivo antitumor activities of GA in mouse NCI-H460 xenograft models. When xenograft tumor mass reached a volume of about 100 mm^3, mice were injected intraperitoneally with 20 mg/kg GA and 8 mg/kg doxorubicin (positive control) or a vehicle control every 4 days. Representative tumors in the xenograft mice treated with or without GA are shown in **Figure 7A**; the treatments of both compounds (GA and doxorubicin) did not alter body weight significantly (data not shown). GA also significantly ($p < 0.01$) decreased by 40% the tumor weight compared to control (**Figure 2B**) as shown in **Figure 2C**. The results indicate that GA induced 16−35% inhibition of tumor growth compared to control after treatment for from 22 to 38 days. In **Figure 2C**, doxorubicin (8 mg/kg) also significantly reduced tumor mass by ~75% after 38 days of treatment. Tumors in treatment groups were significantly smaller than those in the control group.

GA Inhibited Tumor Size in a Xenograft Mouse Model. On the basis of our in vitro studies, we next examined the in vivo antitumor activities of GA in mouse NCI-H460 xenograft models. When xenograft tumor mass reached a volume of about 100 mm^3, mice were injected intraperitoneally with 20 mg/kg GA and 8 mg/kg doxorubicin (positive control) or a vehicle control every 4 days. Representative tumors in the xenograft mice treated with or without GA are shown in **Figure 7A**, and the treatments of both compounds (GA and doxorubicin) did not alter body weight significantly (data not shown). GA also significantly ($p < 0.01$) decreased by 40% the tumor weight compared to control (**Figure 7B**). As shown in **Figure 7C**, GA reduced tumor mass

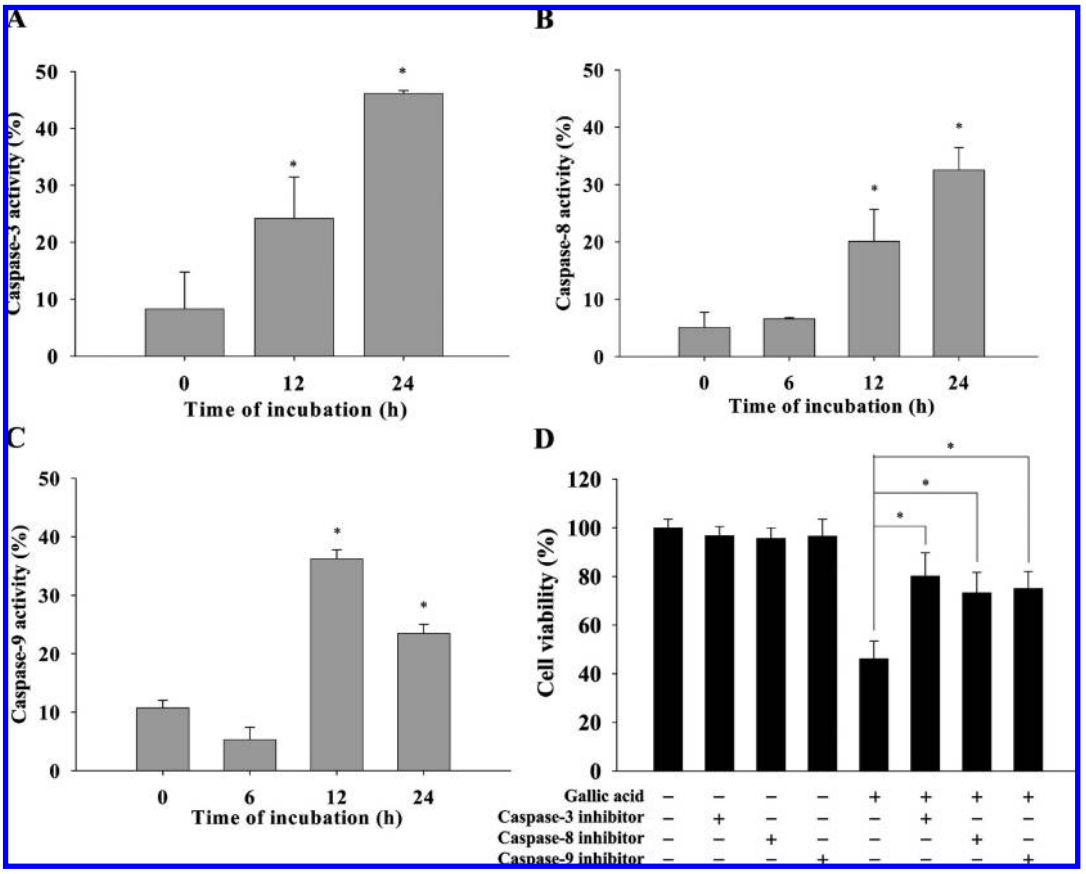

Figure 5. GA affected the activities of caspase-3, -8, and -9 of NCI-H460 cells. Cells were plated onto a 12-well plate in RPMI 1640 medium + 10% FBS, which were preincubated with or without inhibitors and then were incubated with 250 μM GA for 0, 3, 6, 12, and 24 h. Cells were harvested from each sample for caspase-3 (**A**), -8 (**B**), and -9 (**C**), and for percentage of viable cells (**D**), it was determined as described under Materials and Methods. Caspase-3, -8, and -9 activities were determined and analyzed according to the manufacturer's instructions. (**A**) Each experiment was done with triple sets: a, $P < 0.05$, significantly different compared with 0 time treatment by one-way ANOVA. (**B**) Each experiment was done with triple sets: a, $P < 0.05$, significantly different compared with 0 time GA treatment by one-way ANOVA. (**C**) Each experiment was done with triple sets: a, $P < 0.05$, significantly different compared with 0 time treatment by one-way ANOVA. (**D**) Each experiment was done with triple sets: a, $P < 0.05$, significantly different compared with GA treatment by one-way ANOVA.

compared to control after treatment for from 22 to 38 days, and doxorubicin (8 mg/kg) also significantly reduced tumor mass. In **Figure 7D**, GA significantly induced caspase-3, -8, and -9 activities on tumors in the xenograft mice.

DISCUSSION

Gallic acid induced a strong cell growth inhibition, cell cycle arrest, and apoptotic cell death in human prostate cancer DU145 cells in a dose- and time-dependent manner, together with a decrease in cyclin-dependent kinases and cyclins, but strong induction in Cip1/p21, and may go through a caspase-independent pathway (*31*). There have been several studies supporting the anticancer potential of GA (*31*−*33*); however, scientific evidence concerning the mechanism of its active compound(s) is very limited. Here, we showed that GA decreased the percentage of viable NCI-H460 cells and that the effect is in a dose-dependent manner (**Figures 1** and **2**). We also suggest that the anti-NCI-H460 cells of GA were mediated through the regulation of multiple signaling pathways. Our results suggest that GA caused cell death extrinsically along with Fas-associated extrinsic pathway and mitochondrially intrinsic pathways (**Figures 5** and **6**) and, thus, executed cell death as shown by caspase-8, -9, and -3 activation in NCI-H460 cells (**Figure 5D**). Members of the Bcl-2 family were affected, resulting in a pro-apoptotic cell environment. GA may induce apoptosis also through AIF (caspase-independent pathway). Other authors also did not find mitochondria involved gallic acid-induced apoptosis in human prostate carcinoma DU145 cells. Therefore, it may be cell type dependent. Apparently, further investigations are needed.

Two major goals in cancer treatment are the inhibition of survival signaling pathways and induction of apoptosis in cancer cells. Here, our results indicated that GA induced G2/M arrest in NCI-H460 cells, indicating that one of the mechanisms by which GA acts is via inhibition of cell cycle progression. Suppression of the cell cycle in cancer cells has been considered to be one of the most effective strategies for the control of tumor growth (*34*). GA has been reported to interfere with the G2/M phase in colon adenocarcinoma cells (*35*), but GA did not affect cell cycle in other cancer lines (*36*, *37*). Therefore, GA induced cell death or cell cycle arrest may differ depending on the type of cancer cell (*38*). Other factors that may need to be considered are GA concentration and incubation period, which differed in each study.

Our results revealed that GA-induced apoptosis was mainly associated with G2/M phase of the cell cycle in NCI-H460 cells, and it increased the number of apoptotic cells (sub-G1 population) in a dose-dependent manner (**Figure 2B**). We also used DAPI staining to confirm the appearance of apoptotic NCI-H460 cells after exposure to GA (**Figure 3B**). Our results also showed that GA promoted the level of intracellular Ca^{2+} and decreased the levels of $\Delta\Psi_m$, which led to the release of cytochrome *c* from mitochondria. This is in agreement with an earlier study; GA induced apoptosis through generation, Ca^{2+} influx, and activation of calmodulin (*36*).

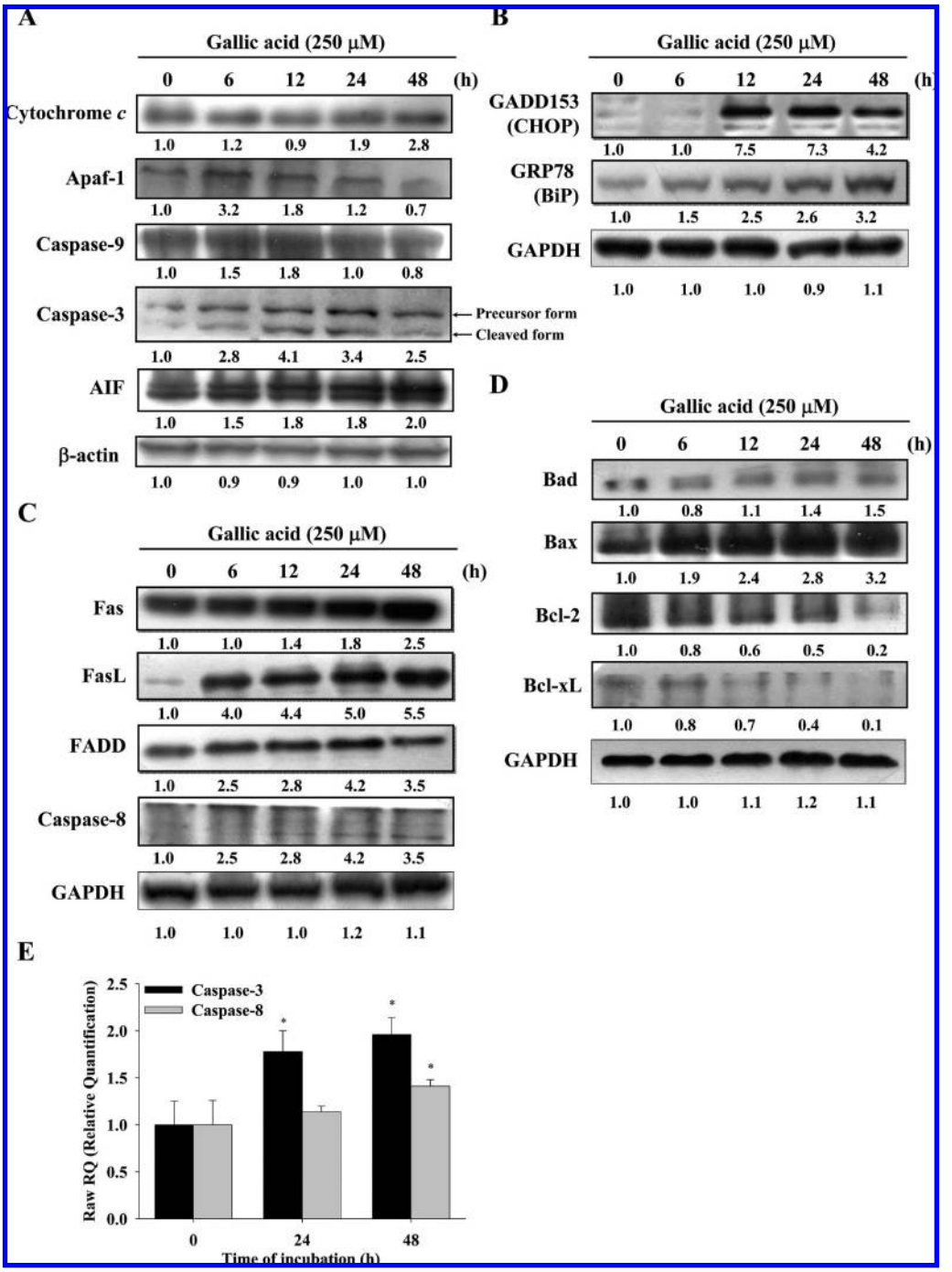

Figure 6. GA affected the apoptotic relative proteins and gene expressions in NCI-H460 cells. A total of 5×10^5 NCI-H460 cells/mL cells were treated with 250 μM GA for 0, 6, 12, 24, and 48 h. Cells were harvested from each sample, and associated proteins were determined by Western blotting. Cytochrome *c*, Apaf-1, AIF, caspase-9, and caspase-3 (**A**), GADD153 and GRP78 (**B**), Fas, FasL, FADD, and caspase-8 (**C**), and Bad, Bax, Bcl-2, and Bcl-xL (**D**) expressions were examined using SDS-PAGE and Western blotting as described under Materials and Methods. The total RNA was extracted from NCI-H460 cells after exposure to GA for 0, 24, and 48 h, and RNA samples were reverse-transcribed cDNA then for real-time PCR. The ratios of *caspase-3* and *-8* mRNA/GAPDH are presented in **E**. Data represent the mean ± SD of three experiments. (**E**) $*$, $P < 0.05$, significantly different compared with 0 h GA treatment by one-way ANOVA.

It is important to elucidate the mechanisms by which GA induces apoptosis in NCI-H460 lung cancer cells to optimize its activity. In the present study, we found that GA induced apoptosis in NCI-H460 lung cancer cells and that this effect is dose dependent. We investigated the contribution of Bcl-2 family proteins to GA-induced apoptosis and found an increase in the expression of Bax protein and a decrease in the expression of Bcl-2 in examined NCI-H460 cells. It is well-known that an increase in the ratio of Bax/Bcl-2 stimulates the release of cytochrome *c* from the mitochondria into the cytosol, promotes activation of caspase-9, and then binds to Apaf-1, leading to the activation of caspase-3 and PARP (*39*, *40*). We found that NCI-H460 cells treated with GA activated caspase-3 in a time-dependent manner, which supports the role of caspase-3 in GA-induced apoptosis. Western blotting also showed that GA promoted the levels of AIF, which means that GA may also induce apoptosis through a caspase-independent pathway (mitochondria-AIF pathway). It was reported that agents can induce apoptosis through

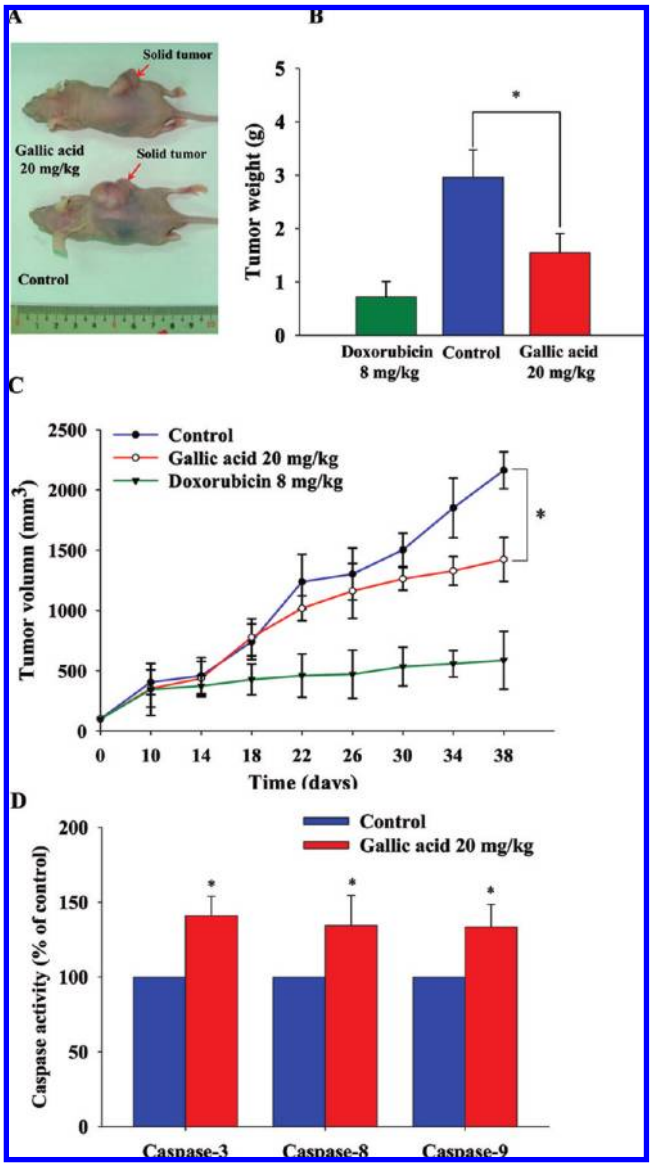

Figure 7. GA inhibited tumor growth on the xenograft animal model. Eighteen athymic BALB/c$^{nu/nu}$ nude mice were s.c. implanted with 1×10^7 NCI-H460 cells for 10 days and then randomly divided into three groups. Group 1 was treated with DMSO only. Group 2 was treated with 20 mg/kg GA, and group 3 was treated with 8 mg/kg doxorubicin. At 34 days, all animals were sacrificed. (**A**) Representative animal with solid tumor; (**B**) tumor weight; (**C**) tumor volume; (**D**) caspase-3, -8, and -9 activities on tumors. Data presented as the mean ± SEM at 10−34 days post-tumor implantation, and the tumor volumes observed in DMSO, doxorubicin, and GA groups were compared as analyzed by one-way ANOVA. Data represent the mean ± SD of six animals. (**B**) ∗, $P < 0.05$, significantly different compared with control by one-way ANOVA. (**C**) ∗, $P < 0.05$, significantly different compared with control by one-way ANOVA.

AIF-mediated caspase-independent mitochondria pathway (*41*). Therefore, natural compounds might have multiple cellular targets to achieve their biological beneficial effects such as tumor growth inhibition (*42*).

In the current study, we showed that GA induces apoptosis in NCI-H460 cells through a caspase-dependent mitochondrial pathway. GA also decreased the weight and size of NCI-H460 cells in xenograft animal models in vivo. The most striking findings are the consistency of effects seen in vitro and in vivo in the present study. GA induced significantly the activities of caspase-3, -8, and -9 in vitro and in vivo. It is well-known that certain products from plants are known to induce apoptosis in tumor cells but not in normal cells (*43*, *44*), and an understanding of the mechanism of those compounds' actions may provide valuable information for their possible application in cancer therapy and prevention. In conclusion, the findings of the present study provide new perspectives for further research on toxicology and pharmacology of GA as a possible candidate for the treatment or prevention of lung cancer.

ABBREVIATIONS USED

$\Delta\Psi_m$, mitochondrial transmembrane potential; DAPI, 4,6-diamidino-2-phenylindole dihydrochloride; DMSO, dimethyl sulfoxide; FBS, fetal bovine serum; GA, gallic acid; PBS, phosphate-buffered saline; PI, propidium iodide; ROS, reactive oxygen species.

LITERATURE CITED

(1) Beckett, W. S. Epidemiology and etiology of lung cancer. *Clin. Chest Med.* **1993**, *14* (1), 1–15.

(2) Gill, R. K.; Vazquez, M. F.; Kramer, A.; Hames, M.; Zhang, L.; Heselmeyer-Haddad, K.; Ried, T.; Shilo, K.; Henschke, C.; Yankelevitz, D.; Jen, J. The use of genetic markers to identify lung cancer in fine needle aspiration samples. *Clin. Cancer Res.* **2008**, *14* (22), 7481–7487.

(3) Cheung, A. F.; Dupage, M. J.; Dong, H. K.; Chen, J.; Jacks, T. Regulated expression of a tumor-associated antigen reveals multiple levels of T-cell tolerance in a mouse model of lung cancer. *Cancer Res.* **2009**, *64* (1), 9–12.

(4) Chiang, T. A.; Chen, P. H.; Wu, P. F.; Wang, T. N.; Chang, P. Y.; Ko, A. M.; Huang, M. S.; Ko, Y. C. Important prognostic factors for the long-term survival of lung cancer subjects in Taiwan. *BMC Cancer* **2008**, *8*, 324.

(5) Lee, C. N.; Yu, M. C.; Bai, K. J.; Chang, J. H.; Fang, C. L.; Hsu, H. L.; Huang, B. S.; Lu, P. C.; Liu, H. E. NAT2 fast acetylator genotypes are associated with an increased risk for lung cancer with wildtype epidermal growth factor receptors in Taiwan. *Lung Cancer* **2008**.

(6) Hong, W. K.; Sporn, M. B. Recent advances in chemoprevention of cancer. *Science* **1997**, *278* (5340), 1073–1077.

(7) AbouEl Hassan, M. A.; Braam, S. R.; Kruyt, F. A. Paclitaxel and vincristine potentiate adenoviral oncolysis that is associated with cell cycle and apoptosis modulation, whereas they differentially affect the viral life cycle in non-small-cell lung cancer cells. *Cancer Gene Ther.* **2006**, *13* (12), 1105–1114.

(8) Yoshioka, K.; Kataoka, T.; Hayashi, T.; Hasegawa, M.; Ishi, Y.; Hibasami, H. Induction of apoptosis by gallic acid in human stomach cancer KATO III and colon adenocarcinoma COLO 205 cell lines. *Oncol. Rep.* **2000**, *7* (6), 1221–1223.

(9) Sakaguchi, N.; Inoue, M.; Ogihara, Y. Reactive oxygen species and intracellular Ca^{2+}, common signals for apoptosis induced by gallic acid. *Biochem. Pharmacol.* **1998**, *55* (12), 1973–1981.

(10) Kawada, M.; Ohno, Y.; Ri, Y.; Ikoma, T.; Yuugetu, H.; Asai, T.; Watanabe, M.; Yasuda, N.; Akao, S.; Takemura, G.; Minatoguchi, S.; Gotoh, K.; Fujiwara, H.; Fukuda, K. Anti-tumor effect of gallic acid on LL-2 lung cancer cells transplanted in mice. *Anticancer Drugs* **2001**, *12* (10), 847–852.

(11) Ohno, Y.; Fukuda, K.; Takemura, G.; Toyota, M.; Watanabe, M.; Yasuda, N.; Xinbin, Q.; Maruyama, R.; Akao, S.; Gotou, K.; Fujiwara, T.; Fujiwara, H. Induction of apoptosis by gallic acid in lung cancer cells. *Anticancer Drugs* **1999**, *10* (9), 845–851.

(12) Sheu, M. J.; Huang, G. J.; Wu, C. H.; Chen, J. S.; Chang, H. Y.; Chang, S. J.; Chung, J. G. Ethanol extract of *Dunaliella salina* induces cell cycle arrest and apoptosis in A549 human non-small cell lung cancer cells. *In Vivo* **2008**, *22* (3), 369–378.

(13) Lu, H. F.; Chen, Y. S.; Yang, J. S.; Chen, J. C.; Lu, K. W.; Chiu, T. H.; Liu, K. C.; Yeh, C. C.; Chen, G. W.; Lin, H. J.; Chung, J. G. Gypenosides induced G0/G1 arrest via inhibition of cyclin E and

induction of apoptosis via activation of caspases-3 and -9 in human lung cancer A-549 cells. *In Vivo* **2008**, *22* (2), 215–221.
(14) Chung, J. G.; Yeh, K. T.; Wu, S. L.; Hsu, N. Y.; Chen, G. W.; Yeh, Y. W.; Ho, H. C. Novel transmembrane GTPase of non-small cell lung cancer identified by mRNA differential display. *Cancer Res.* **2001**, *61* (24), 8873–8879.
(15) Lee, J. H.; Li, Y. C.; Ip, S. W.; Hsu, S. C.; Chang, N. W.; Tang, N. Y.; Yu, C. S.; Chou, S. T.; Lin, S. S.; Lino, C. C.; Yang, J. S.; Chung, J. G. The role of Ca^{2+} in baicalein-induced apoptosis in human breast MDA-MB-231 cancer cells through mitochondria- and caspase-3-dependent pathway. *Anticancer Res.* **2008**, *28* (3A), 1701–1711.
(16) Lin, S. S.; Huang, H. P.; Yang, J. S.; Wu, J. Y.; Hsia, T. C.; Lin, C. C.; Lin, C. W.; Kuo, C. L.; Gibson Wood, W.; Chung, J. G. DNA damage and endoplasmic reticulum stress mediated curcumin-induced cell cycle arrest and apoptosis in human lung carcinoma A-549 cells through the activation caspases cascade- and mitochondrial-dependent pathway. *Cancer Lett.* **2008**, *272* (1), 77–90.
(17) Li, Y. C.; Lin, H. J.; Yang, J. H.; Yang, J. S.; Ho, H. C.; Chang, S. J.; Hsai, T. C.; Lu, H. F.; Huang, A. C.; Chung, J. G. Baicalein-induced apoptosis via endoplasmic reticulum stress through elevations of reactive oxygen species and mitochondria dependent pathway in mouse-rat hybrid retina ganglion cells (N18). *Neurochem. Res.* **2009**, *34* (3), 418–429.
(18) Wang, S. C.; Chung, J. G.; Chen, C. H.; Chen, S. C. 2- and 4-Aminobiphenyls induce oxidative DNA damage in human hepatoma (Hep G2) cells via different mechanisms. *Mutat. Res.* **2006**, *593* (1−2), 9–21.
(19) Chen, J. C.; Lu, K. W.; Tsai, M. L.; Hsu, S. C.; Kuo, C. L.; Yang, J. S.; Hsia, T. C.; Yu, C. S.; Chou, S. T.; Kao, M. C.; Chung, J. G.; Gibson Wood, W. Gypenosides induced G0/G1 arrest via CHk2 and apoptosis through endoplasmic reticulum stress and mitochondria-dependent pathways in human tongue cancer SCC-4 cells. *Oral Oncol.* **2009**, *45* (3), 273–283.
(20) Tsujimura, K.; Ogawara, M.; Takeuchi, Y.; Imajoh-Ohmi, S.; Ha, M. H.; Inagaki, M. Visualization and function of vimentin phosphorylation by cdc2 kinase during mitosis. *J. Biol. Chem.* **1994**, *269* (49), 31097–31106.
(21) Kalbacova, M.; Vrbacky, M.; Drahota, Z.; Melkova, Z. Comparison of the effect of mitochondrial inhibitors on mitochondrial membrane potential in two different cell lines using flow cytometry and spectrofluorometry. *Cytometry A* **2003**, *52* (2), 110–116.
(22) Lu, H. F.; Sue, C. C.; Yu, C. S.; Chen, S. C.; Chen, G. W.; Chung, J. G. Diallyl disulfide (DADS) induced apoptosis undergo caspase-3 activity in human bladder cancer T24 cells. *Food Chem. Toxicol.* **2004**, *42* (10), 1543–1552.
(23) Park, E. K.; Kwon, K. B.; Park, K. I.; Park, B. H.; Jhee, E. C. Role of Ca^{2+} in diallyl disulfide-induced apoptotic cell death of HCT-15 cells. *Exp. Mol. Med.* **2002**, *34* (3), 250–257.
(24) Telford, W. G.; Komoriya, A.; Packard, B. Z. Detection of localized caspase activity in early apoptotic cells by laser scanning cytometry. *Cytometry* **2002**, *47* (2), 81–88.
(25) Yang, J. S.; Chen, G. W.; Hsia, T. C.; Ho, H. C.; Ho, C. C.; Lin, M. W.; Lin, S. S.; Yeh, R. D.; Ip, S. W.; Lu, H. F.; Chung, J. G. Diallyl disulfide induces apoptosis in human colon cancer cell line (COLO 205) through the induction of reactive oxygen species, endoplasmic reticulum stress, caspases casade and mitochondrial-dependent pathways. *Food Chem. Toxicol.* **2009**, *47* (1), 171–179.
(26) Lin, Y. T.; Yang, J. S.; Lin, S. Y.; Tan, T. W.; Ho, C. C.; Hsia, T. C.; Chiu, T. H.; Yu, C. S.; Lu, H. F.; Weng, Y. S.; Chung, J. G. Diallyl disulfide (DADS) induces apoptosis in human cervical cancer Ca Ski cells via reactive oxygen species and Ca2+-dependent mitochondria-dependent pathway. *Anticancer Res.* **2008**, *28* (5A), 2791–2799.
(27) Lai, W. W.; Yang, J. S.; Lai, K. C.; Kuo, C. L.; Hsu, C. K.; Wang, C. K.; Chang, C. Y.; Lin, J. J.; Tang, N. Y.; Chen, P. Y.; Huang, W. W.; Chung, J. G. Rhein induced apoptosis through the endoplasmic reticulum stress, caspase- and mitochondria-dependent pathways in SCC-4 human tongue squamous cancer cells. *In Vivo* **2009**, *23* (2), 309–316.
(28) Hsu, S. C.; Lu, J. H.; Kuo, C. L.; Yang, J. S.; Lin, M. W.; Chen, G. W.; Su, C. C.; Lu, H. F.; Chung, J. G. Crude extracts of Solanum lyratum induced cytotoxicity and apoptosis in a human colon adenocarcinoma cell line (colo 205). *Anticancer Res.* **2008**, *28* (2A), 1045–1054.
(29) Yang, S. F.; Yang, W. E.; Chang, H. R.; Chu, S. C.; Hsieh, Y. S. Luteolin induces apoptosis in oral squamous cancer cells. *J. Dent. Res.* **2008**, *87* (4), 401–406.
(30) Ho, Y. T.; Yang, J. S.; Lu, C. C.; Chiang, J. H.; Li, T. C.; Lin, J. J.; Lai, K. C.; Liao, C. L.; Lin, J. G.; Chung, J. G. Berberine inhibits human tongue squamous carcinoma cancer tumor growth in a murine xenograft model. *Phytomedicine* **2009**.
(31) Agarwal, C.; Tyagi, A.; Agarwal, R. Gallic acid causes inactivating phosphorylation of cdc25A/cdc25C-cdc2 via ATM-Chk2 activation, leading to cell cycle arrest, and induces apoptosis in human prostate carcinoma DU145 cells. *Mol. Cancer Ther.* **2006**, *5* (12), 3294–3302.
(32) Kanai, S.; Okano, H. Mechanism of the protective effects of sumac gall extract and gallic acid on the progression of CCl_4-induced acute liver injury in rats. *Am. J. Chin. Med.* **1998**, *26* (3−4), 333–341.
(33) Sakagami, H.; Yokote, Y.; Akahane, K. Changes in amino acid pool and utilization during apoptosis in HL-60 cells induced by epigallocatechin gallate or gallic acid. *Anticancer Res.* **2001**, *21* (4A), 2441–2447.
(34) Nam, W.; Tak, J.; Ryu, J. K.; Jung, M.; Yook, J. I.; Kim, H. J.; Cha, I. H. Effects of artemisinin and its derivatives on growth inhibition and apoptosis of oral cancer cells. *Head Neck* **2007**, *29* (4), 335–340.
(35) Salucci, M.; Stivala, L. A.; Maiani, G.; Bugianesi, R.; Vannini, V. Flavonoids uptake and their effect on cell cycle of human colon adenocarcinoma cells (Caco2). *Br. J. Cancer* **2002**, *86* (10), 1645–1651.
(36) Inoue, M.; Suzuki, R.; Koide, T.; Sakaguchi, N.; Ogihara, Y.; Yabu, Y. Antioxidant, gallic acid, induces apoptosis in HL-60RG cells. *Biochem. Biophys. Res. Commun.* **1994**, *204* (2), 898–904.
(37) Hsu, C. L.; Huang, S. L.; Yen, G. C. Inhibitory effect of phenolic acids on the proliferation of 3T3-L1 preadipocytes in relation to their antioxidant activity. *J. Agric. Food Chem.* **2006**, *54*, 4191–4197.
(38) Serrano, A.; Palacios, C.; Roy, G.; Cespon, C.; Villar, M. L.; Nocito, M.; Gonzalez-Porque, P. Derivatives of gallic acid induce apoptosis in tumoral cell lines and inhibit lymphocyte proliferation. *Arch. Biochem. Biophys.* **1998**, *350* (1), 49–54.
(39) Bossy-Wetzel, E.; Green, D. R. Caspases induce cytochrome *c* release from mitochondria by activating cytosolic factors. *J. Biol. Chem.* **1999**, *274* (25), 17484–17490.
(40) Pandey, P.; Saleh, A.; Nakazawa, A.; Kumar, S.; Srinivasula, S. M.; Kumar, V.; Weichselbaum, R.; Nalin, C.; Alnemri, E. S.; Kufe, D.; Kharbanda, S. Negative regulation of cytochrome *c*-mediated oligomerization of Apaf-1 and activation of procaspase-9 by heat shock protein 90. *EMBO J.* **2000**, *19* (16), 4310–4322.
(41) Lorenzo, H. K.; Susin, S. A. Therapeutic potential of AIF-mediated caspase-independent programmed cell death. *Drug Resist. Update* **2007**, *10* (6), 235–255.
(42) Cucciolla, V.; Borriello, A.; Oliva, A.; Galletti, P.; Zappia, V.; Della Ragione, F. Resveratrol: from basic science to the clinic. *Cell Cycle* **2007**, *6* (20), 2495–2510.
(43) Hirano, T.; Abe, K.; Gotoh, M.; Oka, K. Citrus flavone tangeretin inhibits leukaemic HL-60 cell growth partially through induction of apoptosis with less cytotoxicity on normal lymphocytes. *Br. J. Cancer* **1995**, *72* (6), 1380–1388.
(44) Chiao, C.; Carothers, A. M.; Grunberger, D.; Solomon, G.; Preston, G. A.; Barrett, J. C. Apoptosis and altered redox state induced by caffeic acid phenethyl ester (CAPE) in transformed rat fibroblast cells. *Cancer Res.* **1995**, *55* (16), 3576–3583.

Received April 22, 2009. Revised manuscript received July 9, 2009. Accepted July 9, 2009. This work was supported by Grant CMU96-086 from China Medical University, Taichung, Taiwan.